Plot-scale assessment of soil freeze/thaw detection and variability with impedance probes: implications for remote sensing validation networks

Matthew Williamson, Justin R. Adams, Aaron A. Berg, Chris Derksen, Peter Toose and Anne Walker

ABSTRACT

Several large in-situ soil moisture-monitoring networks currently exist over seasonally frozen regions that may have use for the validation of remote sensing soil freeze/thaw (F/T) products. However, further understanding of how the existing network instrumentation responds to changes in near surface soil F/T is recommended. This case study describes the results of a small plot-scale (7×7 m) study from November 2013 through April 2014 instrumented with 36 impedance probes. Soil temperature and real dielectric permittivity (ϵ_r') were measured every 15 minutes during F/T transition periods at shallow soil depths (0–10 cm). Categorical soil temperature and real dielectric permittivity techniques were used to define the soil F/T state during these periods. Results demonstrate that both methods for detecting soil F/T have strong agreement (84.7–95.6%) during the fall freeze but weak agreement (53.3–60.9%) during the spring thaw. Bootstrapping results demonstrated both techniques showed a mean difference within $\pm 1.0\,^{\circ}$C and $\pm 1.4\ \epsilon_r'$ between the standard 5 cm below surface measurement depth and probes at 2, 10 and integrated 0–5.7 cm depths installed within the same study plot. Overall this study demonstrates that the Hydra Probe offers promise for near surface soil F/T detection using existing soil moisture monitoring networks particularly for the fall freeze.

Key words | frozen soils, Hydra Probe, impedance probes, remote sensing, soil freeze/thaw, soil moisture probes

Matthew Williamson
Aaron A. Berg (corresponding author)
Department of Geography,
University of Guelph,
Guelph, ON,
N1G2W1, Canada
E-mail: aberg@uoguelph.ca

Justin R. Adams
Wilfrid Laurier University,
Waterloo,
Canada

Chris Derksen
Peter Toose
Anne Walker
Climate Research Division, Environment and
　Climate Change Canada,
Toronto, ON,
M3H 5T4, Canada

INTRODUCTION

The seasonal occurrence of vadose zone soil freezing and thawing (F/T) has a major control on land-surface hydrology and climate over seasonally frozen regions (Hayashi 2013). Freezing soils are characterized by a phase change of liquid water content to ice in response to air and ground temperatures at or below 0 °C. Over seasonally frozen regions, monitoring the timing and extent of F/T is especially critical for predicting spring runoff and soil infiltration capacity (Gray et al. 2001) and for soil-atmosphere biogeochemical cycling (Wagner-Riddle et al. 2017). Monitoring F/T over large scales is complex due to the

heterogeneity of soil and landscape factors as well as atmospheric forcing which in turn influences the timing and depth of soil F/T.

Remote sensing studies have been conducted at microwave frequencies to understand the response of radar backscatter (e.g. Podest et al. 2014; Du et al. 2015) and radiometer brightness temperatures (T_b) (e.g. Zhao et al. 2011; Rautiainen et al. 2014; Roy et al. 2017) to soil F/T. Microwave response to non-frozen soils is strongly influenced by the dielectric permittivity (ε_r*) which is directly related to the amount of liquid water (e.g. $\varepsilon_r* = 80$, distilled water at

20 °C and frequency 50 MHz-5 GHz) held in near-surface soil layers and is distinct from air ($\varepsilon_{r*} = 1$) or dry soil media ($\varepsilon_{r*} = 3$–5) (Ulaby *et al.* 1986; Seyfried & Murdock 2004). As liquid soil water content freezes the free rotation of water molecules is impeded and ε_{r*} is reduced to resemble that of dry soil. This dramatic change in dielectric permittivity can be observed in radar measured backscatter intensities and radiometer measured brightness temperatures (Wegmuller 1990). NASA's L-band (1.41 GHz) Soil Moisture Active Passive (SMAP) mission is producing daily binary F/T classification of near-surface soils (depth <5 cm) for land areas north of 45N (Entekhabi *et al.* 2010). The target accuracy of the SMAP F/T product is 80% (Dunbar *et al.* 2014). Because the SMAP radar experienced a major anomaly in July 2015, F/T retrievals will continue to be produced from the radiometer data stream at a coarser spatial resolution of 36 kilometers.

With the launch of SMAP, extensive post-launch validation is necessary for confirmation of the satellite's F/T product in order to achieve the mission's accuracy target. A review of F/T studies suggests that remote sensing validation is typically conducted using many different techniques such as frost tubes (Rautiainen *et al.* 2012), land surface models (Bateni *et al.* 2015), air temperature (Colliander *et al.* 2012), proxy data (e.g. CO_2 eddy flux towers and Normalized Difference Vegetation Index (NDVI) images) (Kim *et al.* 2012), soil temperature (Du *et al.* 2015) and soil moisture probes (Khaldoune *et al.* 2011). Although many techniques exist for the validation of remote sensing F/T products, the most common in-ground approaches use soil temperature and soil moisture probes. Typical remote sensing soil F/T validations use in-situ air or soil temperature measurements and a threshold of 0 °C to identify frozen soils (Podest *et al.* 2014; Roy *et al.* 2015; McColl *et al.* 2016). This allows for soils to be classified into a binary F/T state which then can be compared to the satellite retrievals. The second, slightly less common approach uses soil moisture probes which measure the dielectric permittivity of a soil volume. These devices consider the soil freeze/thaw state based on the distinct decrease and increase in the dielectric permittivity of the soil measured during the freezing and thawing process (Watanabe & Wake 2009).

Currently there are a number of large-scale soil moisture monitoring networks which exist over North America that have potential to be used for F/T validation (e.g. Champagne *et al.* 2016; Colliander *et al.* 2017). These networks are instrumented with soil moisture probes which measure the dielectric permittivity (also known as the complex dielectric permittivity) of a soil volume. The dielectric permittivity is defined by real (ε_r') and imaginary (ε_r) components. Typically, most devices used at these networks rely exclusively on the real component due to the established relationship between ε_r' and volumetric soil moisture (Topp *et al.* 1980). However, these networks do not typically utilize ε_r' measurements during the winter period, although these measurements have potential application for the soil F/T detection. Specifically, soil moisture probes are able to detect soil freezing or thawing by the change in real dielectric permittivity that occurs at 0 °C. This distinct signal is then reclassified using a thresholding approach which involves a site specific ε_r' threshold for frozen and thawed soils. Typically, a real dielectric permittivity threshold of a frozen soil is between 3–10, and 15–30 for a thawed soil (Watanabe & Wake 2009; Rautiainen *et al.* 2014; Du *et al.* 2015).

In Canada, there are two soil moisture networks particularly well suited for F/T validation: (1) the Environment Canada/University of Guelph network in the Brightwater Creek watershed in Saskatchewan (36 stations) and (2) the Agriculture and Agri-food Canada network in the Brunkild sub-watershed in Manitoba (nine stations) (Champagne *et al.* 2016). Both networks are currently used for satellite soil moisture product validation for missions such as SMAP (Colliander *et al.* 2017), the Advanced Microwave Scanning Radiometer-2, and the Soil Moisture and Ocean Salinity mission. The networks consist of monitoring stations established in or adjacent to agricultural fields, each utilizing a profile of permanently installed Stevens Hydra Probe II soil moisture sensors (also referred to as the Hydra Probe). The Hydra Probes measure soil temperature and real dielectric permittivity, installed at standard World Meteorological Organization (WMO) soil monitoring depths of 5, 20, and 50 cm below ground (Dorigo *et al.* 2011). Over the United States there is also potential to utilize a number of soil moisture networks for F/T validation. Specifically, the Snow Telemetry (381 stations), Soil Moisture Analysis Network (182 stations) and US Climate Reference Network (113 stations) could also provide a broad-scale

validation of satellite F/T products across much of Alaska and north-western or north-eastern United States (Dorigo *et al.* 2011). These networks are also instrumented with the Hydra Probe at standard World Meteorological Organization instrument depths. Like the Canadian networks, soil moisture probe data from these networks are largely under-utilized during F/T periods and during the winter, yet there is obvious potential to utilize Hydra Probe observations in support of satellite F/T validation (i.e. SMAP).

The use of time-domain reflectometry, frequency-domain reflectometry and impedance devices has been investigated for use in soil freezing conditions (Spaans & Baker 1995, 1996; Yoshikawa & Overduin 2005; Watanabe & Wake 2009; Kelleners & Norton 2012; He & Dyck 2013). Although the Hydra Probe has been evaluated for use under soil freezing conditions, there are two key uncertainties related to the application of the Hydra Probe for validation of F/T remote sensing products. First of all, categorical F/T signals produced from the Hydra Probe using both a soil temperature threshold and real dielectric permittivity (hereafter referred to as real dielectric) measurements have not been thoroughly evaluated or compared. The second uncertainty regarding in-situ validation of remote sensing F/T products is the 5 cm below ground standard installation depth of the Hydra Probe at existing soil moisture monitoring networks. The penetration depth of the L-band wavelength used by satellites such as SMAP for soil moisture retrievals was found to be ~2 cm, with drier soils potentially having deeper penetration (Escorihuela *et al.* 2010). Determining if a discrepancy in soil temperature and real dielectric exists between the standard 5 cm horizontal probe installation and the near surface (0–5 cm) soil properties is important to ensure that satellite F/T product validation can be corroborated with representative in-situ observations. If a significant difference exists in the soil temperature and real dielectric in the near surface soil layers (0–5 cm), this may contribute to F/T classification errors using the network standard 5 cm instrument depth.

With this in mind, the purpose of this study is to examine soil temperature and real dielectric observations from near-surface soil layers over a small research plot to address two main research objectives with implications for prospective microwave satellite F/T validation using current soil moisture networks:

1. Assess and compare the sensitivity and performance of Hydra Probe soil temperature and real dielectric approaches for detecting soil F/T.
2. Examine the inter-sensor variance of Hydra Probe soil temperature and real dielectric measurements within a small plot at different near-surface depths relative to the WMO standard soil monitoring network probe installation depth of 5 cm below ground.

MATERIALS AND METHODS

Description of Stevens Hydra Probe II soil moisture sensor

The Stevens Hydra Probe II is designed primarily for the measurement of soil dielectric permittivity, electrical conductivity and temperature and is one of the most commonly used devices in soil moisture networks worldwide (Dorigo *et al.* 2013). The most common application of these sensors is to monitor soil moisture (Stevens Water Content Monitoring 2007). The Hydra Probe sensor has four metal tines, each approximately 5.7 cm in length and 0.3 cm in diameter, for an integrated measurement diameter of 2.4 cm (Vaz *et al.* 2013). It operates by transmitting a 50 MHz radio wave along the length of the metal tines and in turn measures the reflection of this standing wave in the form of three voltages. These raw voltages received by the sensor are based on impedance properties of the probe and dielectric permittivity (ε_{r*}) of the soil media (Seyfried & Grant 2007). Voltages and the impedance of a probe are then used to calculate dielectric permittivity ($\varepsilon_r^{'}$ and ε_r) values using internal manufacturer conversions described in detail in Kelleners *et al.* (2009). Although both $\varepsilon_r^{'}$ and ε_r are measured by the Hydra Probe, $\varepsilon_r^{'}$ is the focus of this study since ε_r is a loss term and not typically reported. The accuracy of real ($\varepsilon_r^{'}$) dielectric measurements is ±0.5 or ±1% (whichever is greater), although the instrument is known to show a high degree of precision as documented in a study by Seyfried & Murdock (2004).

The Hydra Probe measures soil temperature from two different thermistors. A diode thermistor is located inside the head of the instrument while the other is on the exposed faceplate of the instrument. The thermistor located inside

the casing of the instrument was not included in the study as it is less representative of true soil temperature since the thermistor is not in direct contact with the soil and is not commonly logged in the large-scale Canadian soil monitoring networks. Instead, temperatures in this study are measured from the thermistor on the faceplate of the Hydra Probe. These measurements are internally calibrated and do not require further processing. The accuracy of these temperature data is reported to be $\pm 0.6\,°C$ (Stevens Water Content Monitoring 2007).

Numerous field and laboratory studies have been conducted to describe reliability and calibration of the Hydra Probe for soil moisture determination (Seyfried *et al.* 2005). Volumetric soil moisture can accurately be determined using Hydra Probe's real dielectric measurements via laboratory calibrations (Burns *et al.* 2014). In the case of freezing soils, liquid water content may remain depending on the hydraulic and chemical properties of the soil (Hayashi 2013). In these conditions, calibration equations relating ε_r* to water content (e.g. Burns *et al.* 2014) are not transferable for quantifying water content in freezing soils without adding considerable uncertainty (Yoshikawa & Overduin 2005; Kahimba & Ranjan 2007; Seybold *et al.* 2010; Kelleners & Norton 2012). This is because standard dry-down calibration techniques rely on the difference between the dielectric permittivity of water ($\varepsilon_r* = 80$ at $20°C$) and air ($\varepsilon_r* = 1$) rather than the difference between water and ice (($\varepsilon_r* = 3$) (Spaans & Baker 1995). Applying these calibration techniques to frozen soils also presumes that dielectric permittivity is not temperature dependent which could further add to the uncertainty as laboratory calibrations are normally conducted at room temperature (Kahimba & Ranjan 2007). With this in mind volumetric soil moisture measurements were not reported in this study during soil freezing conditions.

Study site

The small plot-scale study was undertaken at Environment and Climate Change Canada's Centre for Atmospheric Research Experiments (CARE) in Egbert, Ontario (44° 14′N, 79° 47′W, 250 m ASL). The CARE site was chosen as it is intensively instrumented for meteorological and soil measurement. The measurements were acquired from November 15, 2013 to April 22, 2014. Over this period, monthly air temperatures were below normal with the exception of November which saw temperatures just slightly above the historic average (Environment Canada 2016). Snow depth was also considerably above historic averages for the 2013–14 winter. The 7×7 m instrumented plot was located on a gently sloping grass covered field. The soil textural class of the footprint was determined to be loamy sand (82.5% sand, 14.75% silt, 2.75% clay) according to hydrometer and mechanical sieve analysis (Bowles 1970).

Site instrumentation

A total of nine Hydra Probe measurement profiles were randomly distributed within the 7×7 m footprint, each consisting of four Hydra Probes (Figure 1). At each profile, three Hydra Probes were installed horizontally (H) in the soil at depths centered at 2, 5 and 10 cm below ground recording an integrated soil measurement from 0.5–3.5, 3.5–6.5 and 8.5–11.5 cm below ground respectively. The fourth Hydra Probe was inserted vertically (V) at the soil surface (0–5.7 cm) measuring an integrated real dielectric measurement over the depths 0–5.7 cm below ground (Adams *et al.* 2013). However, it is important to note that the soil temperature measurement from these vertically installed probes are not integrated over the 0–5.7 cm depths, and instead are more representative of the temperatures at the air/soil interface. Hydra Probe data were recorded to a Stevens Datalogger 3000 at 15 minute intervals during two periods: November 15 to December 18, 2013 (fall freeze) and March 20 to April 22, 2014 (spring thaw). Following the initial recording period, data loggers and batteries were removed to recharge low batteries and prevent damage to equipment over the winter. The Hydra Probes remained installed in the ground undisturbed prior to reconnection to data loggers in March. Seven of the nine stations (28 Hydra Probes) successfully recorded data over the entire study period. Issues with power supply (i.e. batteries) compromised the operation of the other two stations. Of note, these power supply issues would not be encountered at permanent monitoring stations which are generally outfitted with re-chargeable power systems.

In addition to the Hydra Probes installed within the footprint, a snow depth sensor, an air temperature sensor,
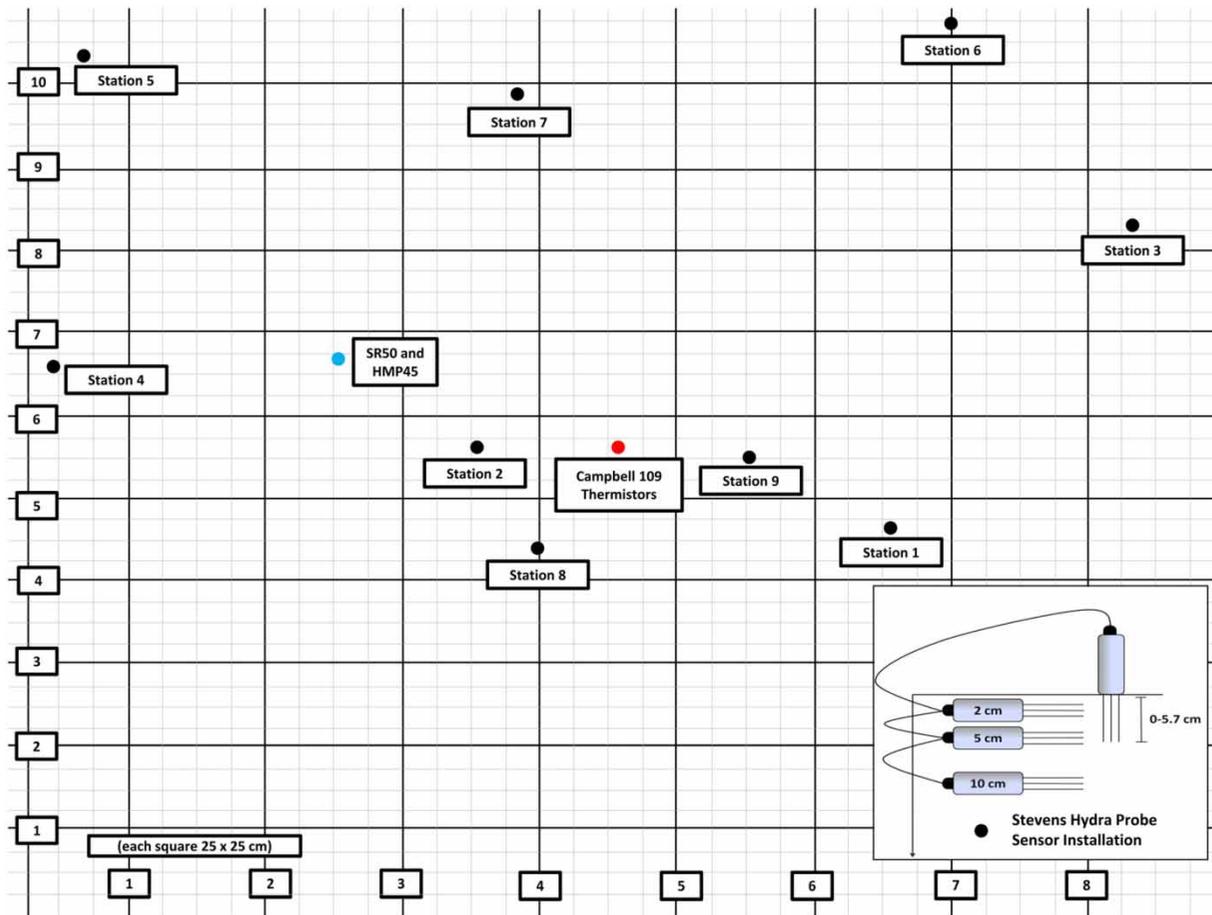
Figure 1 │ Field station schematic and Hydra Probe installation depths (bottom right).

and six additional independent soil temperature sensors were installed roughly in the center of the small plot. These sensors recorded their respective measurements continuously from November 15, 2013 through to April 22, 2014. Snow depth within the site was recorded using a Campbell SR50 sonic ranging snow depth sensor (accuracy: ±1 cm or 0.4%) (Campbell Scientific 2007). Air temperature at the site was recorded using a Campbell HMP45 air temperature sensor (accuracy: ±0.5 °C) located two metres above the soil surface (Campbell Scientific 2004). Six Campbell 109 temperature sensors (accuracy: ±0.25 °C between −10 °C and 70 °C) were installed in the center of the small plot in a single soil profile at depths of 0, 2.5, 5, 10, 20 and 40 cm below ground (Campbell Scientific 2014). The temperature sensor installed at the 5 cm depth malfunctioned for the entire study period.

Data analysis

Soil temperature and real dielectric measurements were compared between Hydra Probes during both transition periods. A sample standard deviation was calculated for each measurement parameter every 15 minutes to determine the inter-sensor variability. This was calculated at each of the four soil instrument depths from all available operational probes during both transition periods. A Kolmogorov-Smirnov test was conducted on the soil temperature and real dielectric measurements for both periods to determine the normality of the datasets. Results of this test were used to determine the appropriate correlation test.

In order to compare soil temperature and real dielectric approaches for F/T detection, individual probes were classified categorically into a binary frozen or thawed state.

Previously, several remote sensing studies applied a soil temperature threshold of 0 °C to classify frozen/unfrozen conditions (Kimball *et al.* 1999; Khaldoune *et al.* 2011; Colliander *et al.* 2012; Podest *et al.* 2014). Previous work by Watanabe & Wake (2009) showed that their dielectric mixing model was most effective in sandy soils and resulted in soils experiencing a sharp decrease in real dielectric between 0 and −0.01 °C. However, the study also noted that volumetric water contents decreased more gradually between 0 and −10 °C in finer textured soils, suggesting that a threshold of 0 °C is likely to be less robust in these soil types. With the low electrical conductivities found and the coarse texture of the soil (loamy sand) a soil freezing threshold of 0 °C was chosen for this study.

Examining the soil's electrical conductivity is important as the presence of soluble salts such as sodium have been shown to affect the temperature at which soils freeze (Drotz *et al.* 2009). Soil electrical conductivities from the Hydra Probes were examined during both transition periods to verify the applicability of this 0 °C threshold. Electrical conductivities from the Hydra Probes were consistently well below 0.11 S/m, suggesting non-saline conditions (Whitney 1998).

Real dielectric data were also used to classify soils as frozen or thawed using a modified seasonal threshold algorithm described in McDonald & Kimball (2005). The modified algorithm compares the time sequence of real dielectric measurements to seasonal reference states of frozen and non-frozen soil conditions for the identification of temporal changes in dielectric permittivity that occur as the soils transition between mainly frozen and non-frozen conditions. The modified seasonal threshold algorithm (Equation (1)) was used where $\Delta(t)$ is a dimensionless scale factor, $\varepsilon_r'(t)$ is the real dielectric at time (t), $\varepsilon_{r'fr}$ is the average real dielectric of frozen soil and $\varepsilon_{r'th}$ is the average real dielectric of thawed soil.

$$\Delta(t) = \frac{\varepsilon_r'(t) - \varepsilon_r'_{fr}}{\varepsilon_r'_{th} - \varepsilon_r'_{fr}} \tag{1}$$

The average real dielectric of thawed soil was determined during a week in early November 2013 when average air temperatures were 6.3 °C and soil temperature at 2 cm was 5.3 °C. Similarly, the real dielectric frozen reference was taken during two weeks in December 2013 when air temperature was −10.4 °C and soil temperature at 2 cm was −0.5 °C. For this study, average real dielectric of frozen and thawed soils were found to be 5 and 14, respectively. These are very similar to thresholds of frozen and thawed real dielectric values found for sand in Watanabe & Wake (2009). Next the scale factor was then used to classify soils as frozen or thawed relative to a threshold (*T*) using Equation (2).

$$\Delta(t) > T (\text{thawed soil})$$
$$\Delta(t) \leq T (\text{frozen soil}) \tag{2}$$

To optimize the F/T threshold (*T*) using the scale factor $\Delta(t)$, an iterative approach was used where the threshold value (*T*) was increased by 0.05 between 0.1 and 0.9. This optimization was conducted for the duration of both transition periods using the footprint averaged soil temperature. More specifically, the binary F/T state produced by the given value of *T* was then compared to the soil temperature (0 cm) F/T state allowing for a percent accuracy to be calculated. The threshold with the highest overall accuracy for the combined soil depths was then chosen. For this study, the best matched F/T threshold (*T*) was found to be 0.75 for the real dielectric measurements using the modified seasonal threshold algorithm. This threshold suggests a slight weighting towards soils being frozen (Podest *et al.* 2014). Caution should be applied to the adoption of the threshold to different soil textures.

Upon classifying all Hydra Probe soil measurements as frozen or thawed using the soil temperature and real dielectric approaches described above, a percent frozen statistic was computed using Equation (3) every 15 minutes from all available stations. The average agreement between the soil temperature and real dielectric binary F/T signal was calculated using Equation (4) for the duration of each period.

$$\% \, \text{Frozen} = \frac{\text{Number of Stations Frozen}}{\text{Total Operational Stations}} \tag{3}$$

$$\% \, \text{Average Agreement} = \frac{\text{Identical Signal}}{\text{Number of Samples}} \tag{4}$$

Correlations (between soil temperature and real dielectric measurements among sensors and sensor depths) were conducted using the Spearman's rank correlation coefficient test as a significant Kolmogorov-Smirnov test indicated a

non-normal distribution. Inter-sensor variability was evaluated between Hydra Probes installed vertically at 0–5.7 cm and horizontally at 2 and 10 cm and depths relative to the horizontal instrument at 5 cm depth. Inter-sensor variability (differences) in soil temperature and real dielectric measurements was assessed during the two transition periods using a bootstrapping procedure. The bootstrapping technique was chosen as it allows robust statistical confidence intervals to be obtained without the need to assume population normality (Good 2006). The bootstrapping process involved randomly sub-sampling 30 uniformly distributed observations from the original dataset, determining the mean difference of each sub-sample and repeating the sampling procedure 1000 times. The mean differences were then ranked so that the 25th and 975th values represented the 95% confidence interval. Lastly, a footprint mean difference was calculated, also using a bootstrapping procedure, where the average of all operational stations within the footprint was determined and then resampled 1000 times with the confidence limits determined as described above.

RESULTS AND DISCUSSION

Summary of data collected over study period

The plot-scale measured variables are summarized in Figure 2. A consistent snowpack was present between December 15 and April 4 with an average depth of 26 cm and a maximum depth of 46 cm recorded on January 7 (Figure 2(a)). Prior to December 15 a shallow and variable snow pack (<10 cm) was observed. Except for several short periods, the air temperature was consistently below 0 °C from November 22 to March 26. Figure 2(a) illustrates the similarity in diurnal and seasonal patterns of temperatures between the air temperature and Campbell thermistors installed in the soil at 0 and 2.5 cm depths before the onset of snow and following snowmelt (Figure 2(a)). Soil temperature measurements were relatively static during periods of snowcover, with temperature values hovering at or just below 0 °C.

The Hydra Probe soil temperature initially matched air temperature fluctuations until approximately November 24 when a shallow snow cover of ~10 cm developed and soil temperatures became less variable. This trend continued until December 5 when a short melting period eliminated snow cover. From December 6 onward, soil temperature at 0, 2 and 5 cm dropped below 0 °C for a continuous period (Figure 2(b)). The vertically installed Hydra Probe (0 cm), which measures air/soil or snow/soil interface temperature, was initially most responsive to freezing air temperatures and was therefore most temporally variable over this period. The temporal variability of each Hydra Probe decreased with increased measurement depth. The real dielectric values during non-freezing conditions in late November and early December varied as a function of soil water content but began to decline from December 6 to 9 generally coinciding with the decreases in soil temperature (after the disappearance of the overlying snow cover), and consistent freezing air temperatures. A site specific real dielectric to volumetric soil water content calibration relationship derived from Burns *et al.* (2014) indicated an average soil moisture of 0.17 $m^3 m^{-3}$ in the period leading up to soil freeze. Following this period real dielectric values were between 5 and 8 which indicated a very dry soil. However, in this case the low real dielectric values were indicative of frozen soils.

Observations of the Hydra Probe soil temperature and real dielectric measurements were less coherent during the thaw period. During the spring thaw, Hydra Probe temperature data for all depths remained relatively static at just below 0 °C until melting approximately between April 5 and 9 (Figure 2(c)). During this period real dielectric data fluctuated between 10 and 15. Unlike in the freeze period where the real dielectric measurements dropped in response to freezing soil temperature, the real dielectric values during the thaw period initially increased from the added liquid water content due to snow melting and then after complete disappearance of the snow cover for a short period fluctuated on a diurnal F/T cycle responding to the freezing and thawing of the soils. These rapid changes were further demonstrated by the larger variability in the real dielectric during the thaw shown in Figure 3(b) where Hydra Probes showed a higher median standard deviation and interquartile range between stations. Of note, Hydra Probe soil temperature standard deviation does not exhibit a similar degree of inter-sensor variability during the spring thaw (Figure 3(a)).
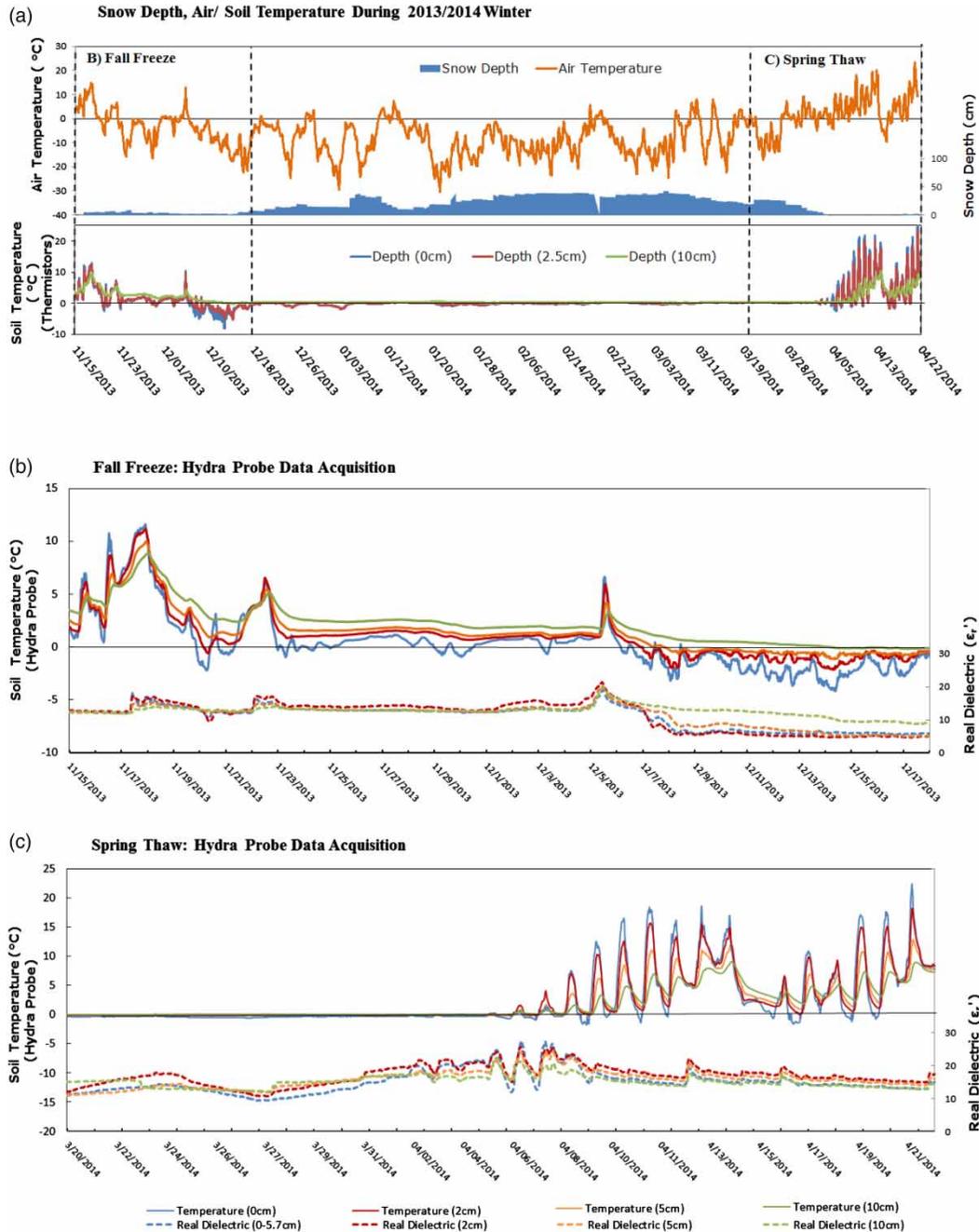
Figure 2 │ (a) Top: air temperature and snow depth from November 15, 2013 to April 22, 2014; bottom: soil temperature at the 0, 2.5 and 10 cm depths recorded by the Campbell thermistors, (b) footprint mean of Hydra Probe measured soil temperature (solid lines) and real dielectric (dashed lines) at 0–5.7, 2, 5 and 10 cm depths during the fall freeze and (c) spring thaw.

Comparison of soil temperature and real dielectric approaches

Significant ($p < 0.01$) correlation (r) results in the fall demonstrated a strong relationship of 0.727, 0.761,

0.714 and 0.497 for the vertical, 2, 5 and 10 cm probes between the soil temperature and real dielectric measurements (Table 1). However, during the spring thaw, correlations showed weak to no relationship between parameters with correlations of 0.332, 0.103, 0.413 and
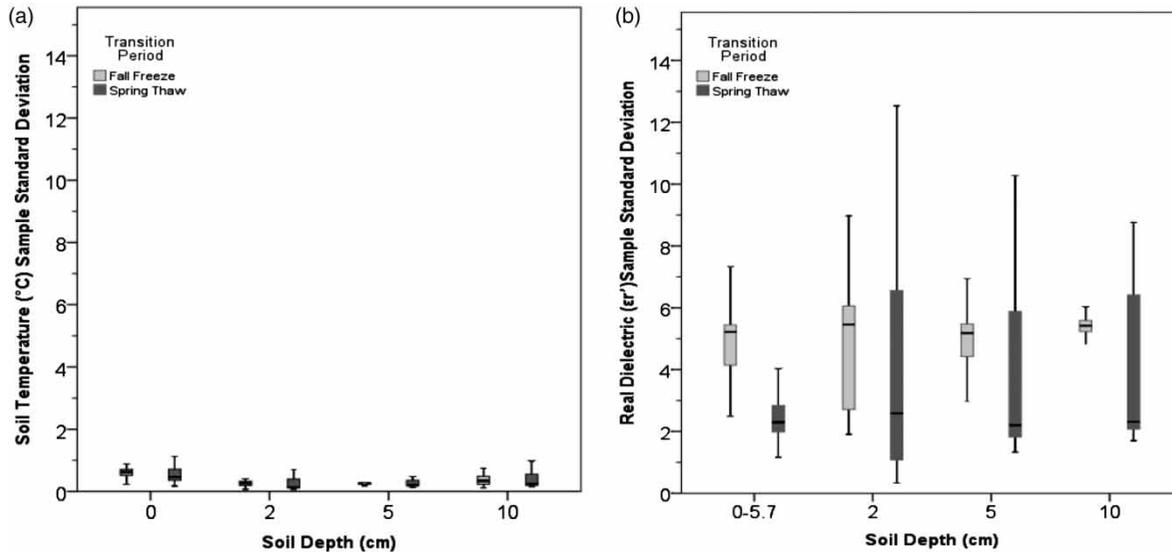
Figure 3 │ Sample standard deviation of all operational Hydra Probes by depth for (a) soil temperature and (b) real dielectric measurements from November 15 to December 18, 2013 (fall freeze) and March 20 to April 22, 2014 (spring thaw) estimated every 15 minutes. The maximum and minimum standard deviation: black whiskers, interquartile range (Q3-Q1) shown as the box and median as a black line.

Table 1 │ Spearman's rank correlation coefficient (*r*) between soil temperature and soil real dielectric during the fall and spring transition periods

Correlation between soil temperature vs real dielectric at soil depths	Fall freeze (*r*) (*n* = 3209)	Spring thaw (*r*) (*n* = 3161)
(A) 0 cm vs. 0–5.7 cm (vertical)	0.727	0.332
(B) 2 cm (horizontal)	0.761	0.103
(C) 5 cm (horizontal)	0.714	0.413
(D) 10 cm (horizontal)	0.497	−0.260

All correlations significant to $p < 0.01$.

−0.260 for the vertical, 2, 5 and 10 cm probes respectively.

Results comparing soil temperature and real dielectric approaches for detecting frozen soils are shown in Figure 4 for the freeze and thaw periods. During the fall freeze, both the soil temperature and real dielectric approaches show a 76.7–95.6% agreement for the four probe depths, with the strength of this agreement weakening as soil depth increases. The highest agreement in the F/T signal is 95.6% in the 2 cm soil depth followed by 93.6% and 84.7% in the 5 and 10 cm horizontal probes. From Figure 4 it is also clear that the soil temperature approach reacts slightly sooner to short (typically diurnal) F/T cycles. Of note, in Figure 4(a) the integrated real dielectric measure

(0–5.7 cm) and the 0 cm temperature show the lowest level of agreement (76.7%) which is likely associated with the depth discrepancy of the measurements.

The agreement between detection methods is considerably weaker in the spring, with agreement ranging between 53.3% and 60.9%. As in the fall, it is again clear that short episodic freeze/thaw cycles were detected using the soil temperature method but are missed by real dielectric measurements. Additionally, it can be seen that the soil temperature method also shows a strong agreement between stations, indicating soils to be consistently frozen until April 9. Interestingly, it is clear that the real dielectric approach indicates that the ground may not be as thoroughly frozen as the temperature approach suggests. This onset of thawing registered by the real dielectric approach is likely a result of snowmelt infiltration on March 29 (Figure 4(b), 4(d), 4(f) and 4(h)). A similar finding in Iwata *et al.* (2010) noted that the onset of snowmelt infiltration also resulted in an increase in soil moisture despite soil temperatures hovering below zero.

During the fall freeze it is evident that both detection methods show a strong agreement across all soil depths. This finding suggests satellite F/T validation may be more robust during the fall freeze using both of these approaches. However, the results show a poor agreement
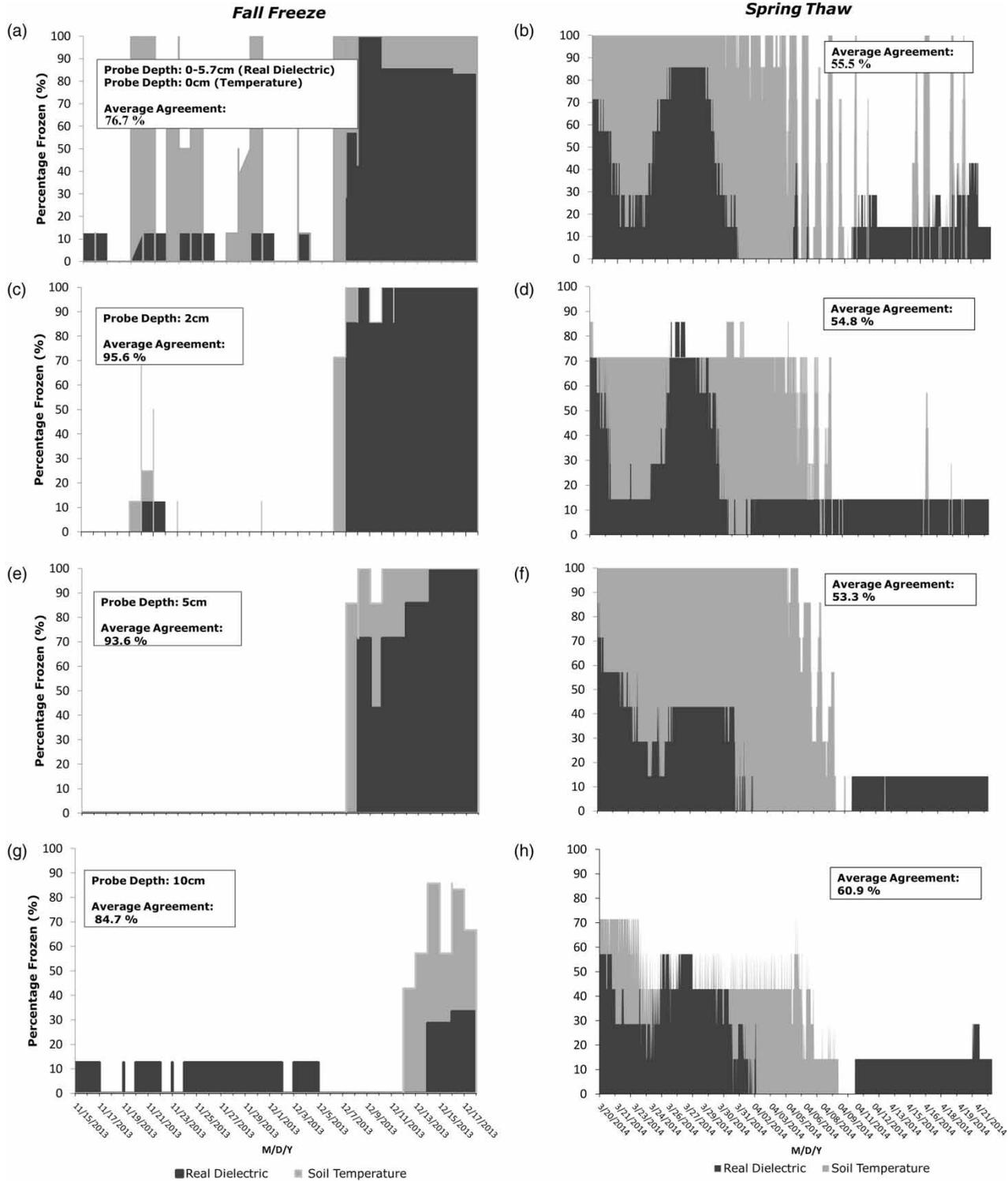
Figure 4 | Soil temperature (gray) and real dielectric (black) and approaches showing percentage of frozen stations (y-axis) during the fall freeze and spring thaw. The percentage of agreement in the soil F/T detection between the two soil temperatures and real dielectric techniques is listed in the legend of each graph. The results for the different sensor depths are illustrated as follows: for the vertical probe (a and b), 2 cm (c and d), 5 cm (e and f) and 10 cm (g and h) soil probes.

in F/T signal between the methods during the spring thaw. This lack of agreement underscores that it may be particularly challenging to accurately validate remote sensing F/T products with the Hydra Probe during this period. Future work should attempt to verify this finding using a small scale radiometer/radar study. Ideally, this future study would address if there is a preferred in-situ validation approach that corresponds best to remote sensing data during transition periods. The finding of this study may further complicate remote sensing F/T retrieval during the spring period which is already challenged due to the influence of wet snow conditions on L-band emission (Roy *et al.* 2015).

The use of a categorical F/T approach using soil temperature and real dielectric has a number of limitations. Foremost, the soil freezing temperature of 0 °C commonly used in remote sensing studies may introduce uncertainty as it assumes soil freezing temperature to be a static threshold and may result in the incorrect categorization of the F/T state during remote sensing validations, as it is very likely that water will be in both liquid and solid form at this threshold temperature. It is still nonetheless important to underscore that this threshold may vary depending on the properties of the soil (Drotz *et al.* 2009; Colliander *et al.* 2012; He & Dyck 2013). One of the largest sources of uncertainty with regard to using soil temperature measurements to detect the F/T threshold is likely the sensor resolution which can record temperatures within ±0.6 °C level of accuracy which can be the difference between detecting frozen/unfrozen conditions during transition periods. Similar to the soil temperature technique, the real dielectric method also has its limitations. In particular, this technique may result in a false frozen signal during periods in which soils are very dry as seen in Figure 4 (Zhao *et al.* 2011; Bateni *et al.* 2013). This is further complicated by use of a thresholding approach. Further, the real dielectric method may be influenced by water present in frozen soils below 0 °C due to increasing capillary and adsorptive forces as soil water freezes (Miller 1980; Spaans & Baker 1996). This is especially true for soil temperatures between −1 and 0 °C where liquid soil water content is changing rapidly (Roth & Boike 2001; Watanabe & Wake 2009; Wen *et al.* 2012).

Mean differences between Hydra Probe measurements relative to 5 cm depth

Figure 5 shows the mean difference in soil temperature between the 0, 2 and 10 cm probes relative to the shallowest network standard depth of 5 cm. During the fall freeze a mean difference of 1.0 °C, 0.3 °C and −0.7 °C was noted between the vertical, 2 and 10 cm probes relative to the network standard 5 cm. Conversely, in the spring period these trends are reversed. This is denoted by a mean difference of −0.4 °C, −0.5 °C and 0.1 °C respectively. The soil temperature bootstrapping results shown in Figure 5 indicate that soil temperatures are relatively homogenous throughout the small-scale 7 m × 7 m plot, though it was apparent that there are slight variations in soil temperature with depth. Comparisons between individual stations and the plot average show that 20/21 and 21/21 stations were within the soil temperature confidence interval during the fall freeze and the spring thaw respectively (Figure 5). It was also evident that soil temperatures were slightly more variable during the spring thaw, denoted by the larger confidence interval. Overall, the mean differences during both transition periods were all within ±1 °C with the majority of differences well inside the sensor resolution of ±0.6. This homogenous nature of soil temperature across meter-scale study plots has also been noted in Iwata *et al.* (2010).

Results from the real dielectric bootstrapping found a mean difference of −0.7, −0.1 and −1.4 ε_r' during the fall freeze and 0.8, −1.2 and 0.7 ε_r' during the spring thaw between the vertical 0–5.7, 2 and 10 cm probes relative to the shallowest network standard depth of 5 cm. This finding suggests that the mean differences in real dielectric measurements from different layer depths are slightly greater than the instrument resolution ($\varepsilon_r' \pm 0.5$ or 1%). It is also apparent from Figure 6 that individual stations show a larger spread relative to the plot average, which suggests that the real dielectric measurements were more variable compared to measured soil temperatures. This is documented during both transition periods where 14 of 21 stations were within the real dielectric confidence interval of the plot average (black and orange stations in Figure 6). It is also clear that the real dielectric was more variable during the spring period, signified by the greater spread between individual stations and the plot average. This finding is also confirmed
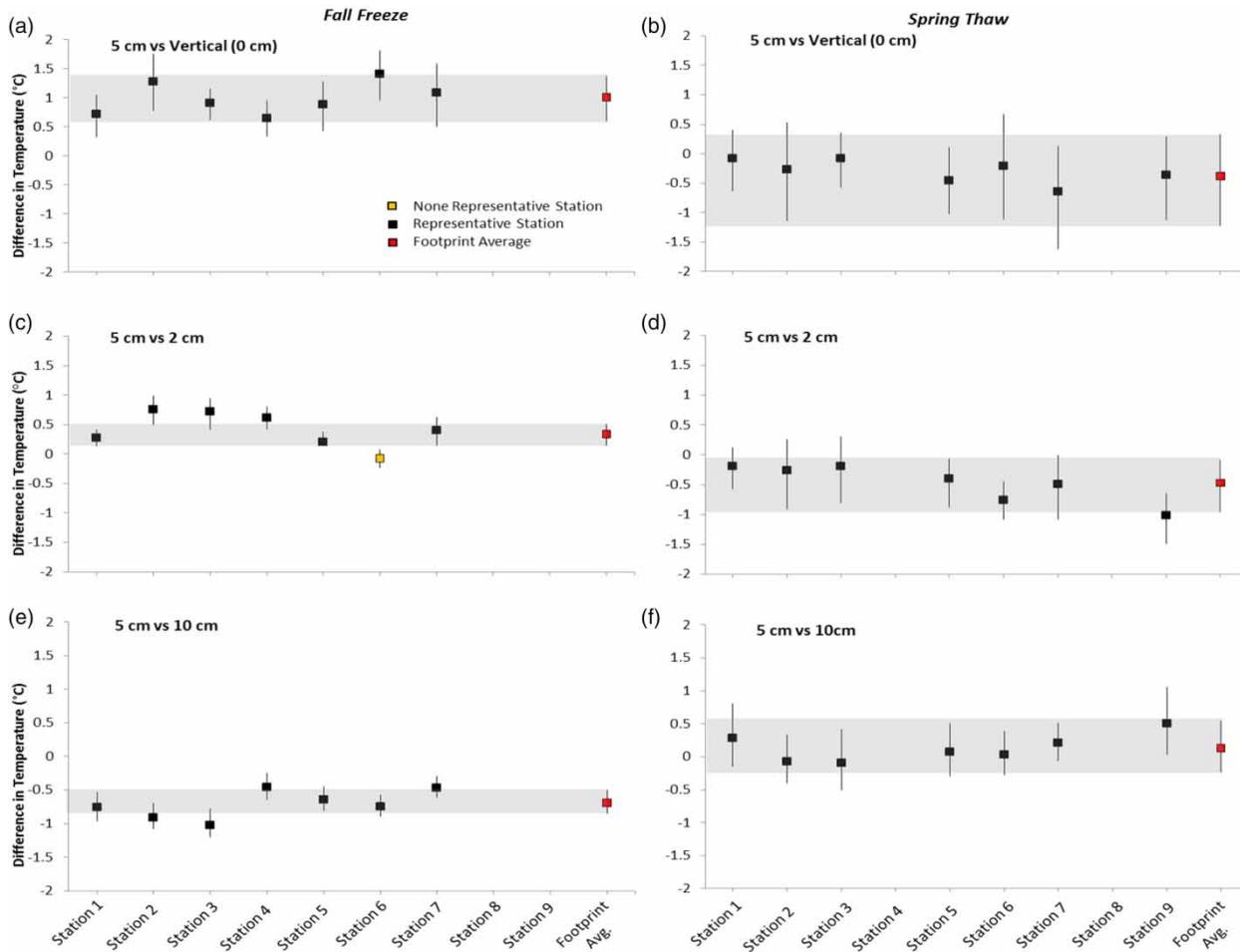
Figure 5 │ Soil temperature bootstrapping results computed for stations one to nine for (a and b) 5 vs 0 cm, (c and d) 5 vs 2 cm and (e and f) 5 vs 10 cm in addition to the footprint (red) during the freeze (left column) and thaw (right column) periods. The rectangles and black vertical lines correspond to the bootstrapping mean and confidence interval of individual stations. The confidence interval of the footprint is denoted above by the shaded gray regions. Please refer to the online version of this paper to see this figure in color: http://dx.doi.org.10.2166/nh.2017.183.

in Figure 3(b) by the larger interquartile range in standard deviation found in the real dielectric during the spring thaw. Finally, it should be noted that stations that were representative of the footprint average during the fall freeze were not necessarily representative during the thaw (Figure 6), again highlighting the spatial complexity of the representation of this process. A study by Iwata *et al.* (2010) also previously documented this same dynamic process of variable influxes in soil moisture due to snow pack melt at small scales. The dynamic and heterogeneous nature of the real dielectric in the plot during both periods has been shown in numerous studies (e.g. Famiglietti *et al.* 2008) which have shown soil moisture to be highly variable even at small scale.

A comparison between the 5 cm network standard probe depth and the vertical (0–5.7) and 2 cm probes for both the soil temperature versus real dielectric techniques for identifying soil F/T dates showed a difference in the timing of soil freezing in the near surface (0–5.7 cm). It was found that the network standard 5 cm horizontal probe may result in the potential misrepresentation of near surface F/T status during the fall freeze by up to 3 days if validating with temperature data, and up to 11 days if validating with real dielectric measurements. Future work should explore this issue in more detail as it remains unclear if this temporal discrepancy also occurred during the spring thaw, as a clear F/T signal was not as obvious.
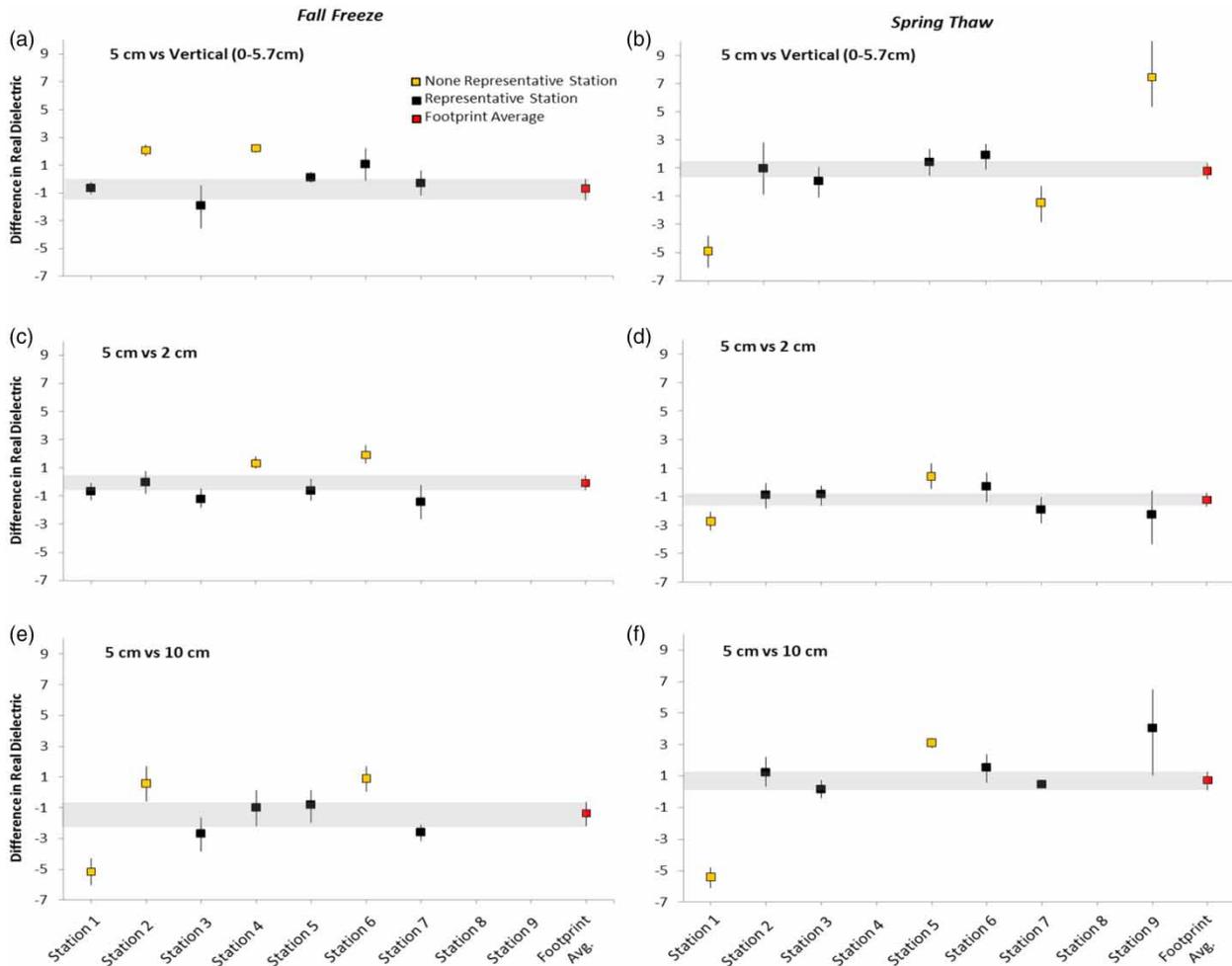
Figure 6 │ Real dielectric bootstrapping results computed for stations one to nine for (a and b) 5 vs 0 cm, (c and d) 5 vs 2 cm and (e and f) 5 vs 10 cm in addition to the footprint (red) during the freeze (left column) and thaw (right column) periods. The rectangles and black vertical lines correspond to the bootstrapping mean and confidence interval of individual stations. The confidence interval of the footprint is denoted above by the shaded gray regions. Please refer to the online version of this paper to see this figure in color: http://dx.doi.org.10.2166/nh.2017.183.

CONCLUSIONS

This research has a number of key implications for the in-situ validation of microwave remote sensing F/T products using the Hydra Probe. Chiefly, the study suggests that both the soil temperature and real dielectric techniques for detecting F/T are reasonably effective during the fall freeze. It is also apparent that during the spring transition period a discrepancy in F/T signal was noted between the methods. This likely means that satellite validation of soil F/T state will be more uncertain during the spring period using the Hydra Probe, especially with the presence of an overlying wet snow which is likely a source of liquid water

in the upper layers of the soil surface, even during periods below $0\,^{\circ}$C soil temperatures. The results of the study also suggest that the real dielectric measurements were slightly more spatially variable than the soil temperature measurements in the footprint. Results from the bootstrapping analysis also show a mean difference of within $\pm 1.0\,^{\circ}$C and $\pm 1.4\varepsilon'_r$ for both soil temperature and real dielectric between the 5 cm horizontal and the 0–5.7, 2 and 10 cm instrument depths, suggesting that the use of the 5 cm network standard depth may result in a small bias in near-surface F/T status. Overall, findings from this study demonstrate that the Hydra Probe offers promise for use in remote sensing soil F/T product validations/calibrations, though

future examination of the device is particularly warranted during the spring thaw.

ACKNOWLEDGEMENTS

REFERENCES

Adams, J., Berg, A. & McNairn, H. 2013 Field level soil moisture variability at 6- and 3-cm sampling depths: implications for microwave sensor validation. *Vadose Zone Journal* **12** (3), 1–12. doi:10.2136/vzj2012.0070.

Bateni, M., Huang, C., Margulis, S., Podest, E. & McDonald, K. 2013 Feasibility of characterizing snowpack and the freeze-thaw state of underlying soil using multifrequency active/passive microwave data. *IEEE Transactions on Geoscience and Remote Sensing* **51** (7), 4085–4102. doi: 10.1109/TGRS.2012.2229466.

Bateni, M., Margulis, S., Podest, E. & McDonald, K. 2015 Characterizing snowpack and the freeze-thaw state of underlying soil via assimilation of multifrequency passive/active microwave data: a case study (NASA CLPX 2003). *IEEE Transaction on Geoscience and Remote Sensing* **53** (1), 173–189. doi:10.1109/TGRS.2014.2320264.

Bowles, J. 1970 *Engineering Properties of Soils and Their Measurement.* McGraw-Hill Book Company, USA.

Burns, T., Adams, J. & Berg, A. 2014 Laboratory calibration of the Hydra Probe soil moisture sensor: comparison of infiltration wet-up vs. dry-down. *Vadose Zone Journal* **13** (12), 1–10. doi: 10.2136/vzj2014.07.0081.

Campbell Scientific 2004 *Model HMP45C Temperature and Relative Humidity Probe: Instruction Manual.* Campbell Scientific Inc., Logan, UT.

Campbell Scientific 2007 *SR50 Sonic Ranging Sensor: Instruction Manual.* Campbell Scientific Inc., Logan, UT.

Campbell Scientific 2014 *Model 109 Temperature Probe: Instruction Manual.* Campbell Scientific Inc., Logan, UT.

Champagne, C., Rowlandson, T., Berg, A., Burns, T., L'Heureux, J., Tetlock, E., Adams, J., McNairn, H., Toth, B. & Itenfisu, D. 2016 Satellite surface soil moisture from SMOS and Aquarius: assessment of accuracy for applications in agricultural landscapes. *International Journal of Applied Earth Observation and Geoinformation* **45**, 143–154. doi: 10.1016/j.jag.2015.09.004.

Colliander, A., McDonald, L., Zimmermann, R., Schroeder, R., Kimball, J. & Njoku, E. 2012 Application of QuikSCAT backscatter to SMAP validation planning: freeze/thaw state over ALECTRA sites in Alaska from 2000 to 2007. *IEEE Transactions on Geoscience and Remote Sensing* **50** (2), 461–468. doi:10.1109/TGRS.2011.2174368.

Colliander, A., Jackson, T., Bindlish, R., Chan, S., Das, N., Kim, S., Cosh, M., Dunbar, S., Dang, L., Pashaian, L., Asanuma, J., Berg, A., Rowlandson, T., Bosch, D., Caldwell, T., Caylor, K., Goodrich, D., al Jassar, H., Lopez-Baeza, E., Martínez-Fernández, J., González-Zamora, A., Livingston, S., McNairn, H., Pacheco, A., Moghaddam, M., Montzka, C., Notarnicola, C., Niedrist, G., Pellarin, T., Prueger, J., Pulliainen, J., Rautiainen, K., Ramos, J., Seyfried, M., Starks, P., Su, B., Zeng, Y., van der Velde, R., Thibeault, M., Dorigo, W., Vreugdenhil, M., Walker, J., Wu, X., Monerris-Belda, A., O'Neill, P., Entekhabi, D., Njoku, E. & Yueh, S. 2017 Validation of SMAP surface soil moisture products with core validation sites. *Remote Sensing of Environment* **191**, 215–231. http://dx.doi.org/10.1016/j.rse.2017.01.021.

Dorigo, W., Wagner, W., Hohensinn, R., Hahn, S., Paulik, C., Xaver, A., Gruber, A., Drusch, M., Mecklenburg, S., van Oevelen, P., Robock, A. & Jackson, T. 2011 The international soil moisture network: a data hosting facility for global in situ soil moisture measurements. *Hydrology Earth System Science* **15**, 1675–1698. doi: 10.5194/hess-15-1675-2011.

Dorigo, W., Xaver, X., Vreughenhil, M., Gruber, A., Hegyiova, A., Sanchis-Dufau, A., Zamojski, D., Cordes, C., Wagner, W. & Drusch, M. 2013 Global automated quality control of in situ moisture data from the international soil moisture network. *Vadose Zone Journal* **12**, 1–21. doi: 10.2136/vzj2012.0097.

Drotz, S., Tilston, E., Sparrman, T., Schleucher, J., Nilsson, M. & Oquist, M. 2009 Contributions of matric and osmotic potentials to the unfrozen water content of frozen soils. *Geoderma* **148**, 392–398. doi: 10.1016/j.geoderma.2008.11.007.

Du, J., Kimball, J., Azarderakhsh, R., Dunbar, S., Moghaddam, M. & McDonald, K. 2015 Classification of Alaska spring thaw characteristics using satellite L-band radar remote sensing. *IEEE Transactions on Geoscience and Remote Sensing* **53** (1), 542–556. doi: 10.1109/TGRS.2014.2325409.

Dunbar, S., Xu, X., Colliander, A., McDonald, K., Podest, E., Njoku, E., Kimball, J., Kim, Y. & Derksen, C. 2014 Soil Moisture Active Passive (SMAP) L3 Radar Freeze/Thaw Product (L3_FT_A). Available from: http://nsidc.org/data/docs/daac/smap/sp_l3_fta/pdfs/D-72549_SMAP%20L3_FT_A%20PSD_10122015_wo-sigs.pdf (accessed 19 May 2016).

Entekhabi, D., Njoku, E., O'Neill, P., Kellogg, K., Crow, W., Edelstein, W., Entin, J., Goodman, S., Jackson, T., Johnson, J., Kimball, J., Piepmeier, J., Koster, R., Martin, N., McDonald, K., Moghaddam, M., Moran, S., Reichle, R., Shi, J., Spencer, M., Thurman, S., Tsang, L. & Zyl, J. 2010 The Soil Moisture Active Passive (SMAP) mission. *Proceedings of the IEEE* **98** (5), 704–716. doi:10.1109/JPROC.2010.2043918.

Environment Canada 2016 *Canadian Climate Normals 1981–2010 Station Data for Egbert CARE, Ontario.* Available from: http://climate.weather.gc.ca/climate_normals/results_1981_2010_e.html?stnID=4397&prov=&lang=e&dCode=5&dispBack=1&StationName=egbert&SearchType=Contains&province=ALL&provBut=Go&month1=0&month2=12 (accessed 19 May 2016).

Escorihuela, M., Chanzy, A., Wigneron, J. & Kerr, Y. 2010 Effective soil moisture sampling depth of L-band radiometry: a case study. *Remote Sensing of Environment* **114** (5), 995–1001. doi: 10.1016/j.rse.2009.12.011.

Famiglietti, J., Ryu, D., Berg, A., Rodell, M. & Jackson, T. 2008 Field observations of soil moisture variability across scales. *Water Resources Research* **44** (1), 1–16. doi: 10.1029/2006WR005804.

Good, P. 2006 *Resampling Methods, A Practical Guide to Data Analysis,* 3rd ed. Birkhauser, Boston, MA.

Gray, D., Toth, B., Zhao, L., Pomeroy, J. & Granger, R. 2001 Estimating areal snowmelt infiltration into frozen soils. *Hydrological Processes* **15**, 3095–3111. doi: 10.1002/hyp.320.

Hayashi, M. 2013 The cold vadose: hydrological and ecological significance of frozen-soil processes. *Vadose Zone Journal* **12** (4), 1–8. doi: 10.2136/vzj2013.03.0064.

He, H. & Dyck, M. 2013 Application of multiphase dielectric mixing models for understanding the effective dielectric permittivity of frozen soils. *Vadose Zone Journal* **12** (1), 1–22. doi: 10.2136/vzj2012.0060.

Iwata, Y., Hayashi, M., Suzuki, S., Hirota, T. & Hasegawa, S. 2010 Effects of snow cover on soil freezing, water movement and snowmelt infiltration: a paired plot experiment. *Water Resources Research* **46** (9), 1–11. doi: 10.1029/2009WR008070.

Kahimba, F. & Ranjan, R. 2007 Soil temperature correction of field TDR readings obtained under near freezing conditions. *Canadian Biosystems Engineering* **49**, 19–26.

Kelleners, T. & Norton, J. 2012 Determining water retention in seasonally frozen soils using hydro impedance sensors. *Soil Science Society of America Journal* **76** (1), 36–50. doi: 10.2136/sssaj 2011.0222.

Kelleners, T., Paige, G. & Gray, S. 2009 Measurement of dielectric properties of Wyoming soils using electromagnetic sensors. *Soil Science Society of America Journal* **73** (5), 1626–1637. doi: 10.2136/sssaj2008.0361.

Khaldoune, J., Bochove, E., Bernier, M. & Nolin, M. 2011 Mapping agricultural frozen soil on the watershed scale using remote sensing data. *Applied and Environmental Soil Science* **2011**, 1–16. doi: 10.1155/2011/193237.

Kim, Y., Kimball, J., Zhang, K. & McDonald, K. 2012 Satellite detection of increasing Northern Hemisphere non-frozen seasons from 1979 to 2008: implications for regional vegetation growth. *Remote Sensing of the Environment* **121**, 472–487. doi: 10.1016/j.rse.2012.02.014.

Kimball, J., McDonald, K., Keyser, A., Frolking, S. & Running, S. 1999 Application of NASA scatterometer (NSCAT) for determining the daily frozen and nonfrozen landscape of Alaska. *Remote Sensing of the Environment* **75**, 113–126. doi: 10.1016/S0034-4257(00)00160-7.

McColl, K., Roy, A., Derksen, C., Konings, A., Alemohammed, S. & Entekhabi, D. 2016 Triple collocation for binary and categorical variables: application to validating landscape freeze/thaw retrievals. *Remote Sensing of Environment* **176**, 31–42. doi: 10.1016/j.rse.2016.01.010.

McDonald, K. & Kimball, J. 2005 Estimation of surface freeze-thaw states using microwave sensors. *Encyclopedia of Hydrologic Sciences* **5** (53), 1–15. doi: 10.1002/0470848944. hsa059a.

Miller, R. 1980 *Applications in Soil Physics: Freezing Phenomena in Soils (In Daniel Hillel Edition).* Academic Press, New York, NY.

Podest, E., McDonald, K. & Kimball, J. 2014 Multisensor microwave sensitivity to freeze/thaw dynamics across a complex boreal landscape. *IEEE Transactions on Geoscience and Remote Sensing* **52** (11), 6818–6828. doi: 10.1109/TGRS. 2014.2303635.

Rautiainen, K., Lemmetyinen, J., Pulliainen, J., Vehvilainen, J., Drusch, M., Kontu, A., Kainulainen, J. & Seppanen, J. 2012 L-band radiometer observations of soil processes in boreal and subarctic environments. *IEEE Transactions on Geoscience and Remote Sensing* **50** (5), 1483–1497. doi: 10. 1109/TGRS.2011.2167755.

Rautiainen, K., Lemmetyinen, J., Schwank, M., Kontu, A., Ménard, C., Mätzler, C., Drusch, M., Wiesmann, A., Ikonen, J. & Pulliainen, J. 2014 Detection of soil freezing from L-band passive microwave observations. *Remote Sensing of Environment* **147**, 206–218. doi: 10.1016/j.rse.2014.03.007.

Roth, K. & Boike, J. 2001 Quantifying the thermal dynamics of a permafrost site near Ny-Alesund, Svalbard. *Water Resources Research* **37** (12), 2901–2914. doi: 10.1029/2000WR000163.

Roy, A., Royer, A., Derksen, C., Brucker, L., Langlois, A., Mialon, A. & Kerr, Y. 2015 Evaluation of spaceborne L-band radiometer measurements for terrestrial freeze/thaw retrievals in Canada. *IEEE Journal of Selected Topics in Applied Earth Observations and Remote Sensing* **99**, 1939–1404. doi: 10.1109/JSTARS.2015.2476358.

Roy, A., Toose, P., Williamson, M., Rowlandson, T., Derksen, C., Royer, A., Berg, A. A., Lemmetyinen, J. & Arnold, L. 2017 Response of L-band brightness temperatures to freeze/thaw and snow dynamics in a prairie environment. *Remote Sensing of Environment.* **191**, 67–80. http://dx.doi.org/10. 1016/j.rse.2017.01.017.

Seybold, C., Balks, M. & Harms, D. 2010 Characterization of active layer water contents in the McMurdo Sound region, Antarctica. *Antarctic Science* **22** (6), 633–645. doi: 10.1017/ S0954102010000696.

Seyfried, M. & Grant, L. 2007 Temperature effects on soil dielectric properties measured at 50 MHz. *Vadose Zone Journal* **6** (4), 759–765. doi: 10.2136/vzj2006.0188.

Seyfried, M. & Murdock, M. 2004 Measurement of soil water content with 50-MHz soil dielectric sensors. *Soil Science Society of America Journal* **68**, 394–403. doi: 10.2136/sssaj2004.3940.

Seyfried, M., Grant, L., Du, E. & Humes, K. 2005 Dielectric loss and calibration of the Hydra Probe soil water sensor. *Vadose Zone Journal* **4**, 1070–1079. doi: 10.2136/vzj2004.0148.

Spaans, E. & Baker, J. 1995 Examining the use of time domain reflectometry for measuring Liquid-d water content in frozen soil. *Water Resources Research* **30** (12), 2917–2925. doi: 10.1029/95WR02769.

Spaans, E. & Baker, J. 1996 The soil freezing characteristic: its measurement and similarity to the soil moisture characteristic. *Soil Science Society of America Journal* **60**, 13–19.

Stevens Water Monitoring Systems Inc. 2007 *The Hydra Probe Soil Sensor: Users Manual.* Stevens Incorporated, Beaverton, OR. Available from: https://www.fondriest.com/pdf/stevens_hydra_manual.pdf (accessed 19 May 2016).

Topp, G., Davis, J. & Annan, A. 1980 Electromagnetic determination of soil water content: measurements in coaxial transmission lines. *Water Resources Research* **16** (3), 574–582.

Ulaby, F., Moore, M. & Fung, A. 1986 *Microwave Remote Sensing, Active and Passive: From Theory to Applications,* Vol. III. Artech House, Norwood, MA.

Vaz, C., Jones, S., Meding, M. & Tuller, M. 2013 Evaluation of standard calibration functions for eight electromagnetic soil moisture sensors. *Vadose Zone Journal* **12** (2), 1–16. doi: 10.2136/vzj2012.0160.

Wagner-Riddle, C., Congreves, K., Abalos, D., Gao, X., Berg, A. A., Brown, S., Thomas Ambadan, J. & Tenuta, M. 2017 Globally important nitrous oxide emissions from croplands induced by freeze-thaw cycles. *Nature Geoscience* **10**, 279–283. doi:10.1038/NGEO2907.

Watanabe, K. & Wake, T. 2009 Measurement of unfrozen water content and relative permittivity of frozen unsaturated soil using NMR and TDR. *Cold Regions Science and Technology* **59**, 34–41. doi: 10.1016/j.coldregions.2009.05.011.

Wegmuller, U. 1990 The effect of freezing and thawing on the microwave signatures of bare soil. *Remote Sensing of the Environment* **33**, 123–135. doi: 10.1016/0034-4257(90)90038-N.

Wen, Z., Ma, W., Feng, W., Deng, Y., Wang, D., Fan, Z. & Zhou, C. 2012 Experimental study on unfrozen water content and soil matric potential of Qinghai-Tibetan silty clay. *Environmental Earth Science* **66**, 1467–1476. doi: 10.1007/s12665-011-1386-0.

Whitney, D. 1998 Soil Salinity, Chapter 12. In: Recommended Chemical Soil Test Procedures for North Central Region: North Central Regional Research Publication No. 211 (Revised). Available from: http://extension.missouri.edu/explorepdf/specialb/sb1001.pdf (accessed 19 May 2016).

Yoshikawa, K. & Overduin, P. 2005 Comparing unfrozen water content measurements of frozen soil using recently developed commercial sensors. *Cold Regions Science and Technology* **42**, 250–256. doi: 10.1016/j.coldregions.2005.03.001.

Zhao, T., Zhang, L., Jiang, L., Zhao, S., Chai, L. & Jin, R. 2011 A new soil freeze/thaw discriminant algorithm using AMSR-E passive microwave imagery. *Hydrological Processes* **25** (11), 1704–1716. doi: 10.1002/hyd.7930.